

# Age-Related Decrease of IF5/BTG4 in Oral and Respiratory Cavities in Mice

Hiroshi Mano,<sup>1\*</sup> Sachie Nakatani,<sup>1</sup> Yoshifumi Kimira,<sup>1</sup> Mikiko Mano,<sup>2</sup> Yuusuke Sekiguchi,<sup>1</sup> Ryang-Hyock Im,<sup>1</sup> Jun Shimizu,<sup>1</sup> and Masahiro Wada<sup>1</sup>

<sup>1</sup>*Faculty of Pharmaceutical Sciences, Josai University, 1-1 Keyakidai, Sakado, Saitama 350-0295, Japan*

<sup>2</sup>*Department of Orthodontics, Meikai University School of Dentistry, 1-1 Keyakidai, Sakado, Saitama 350-0283, Japan*

Received November 12, 2014; Accepted December 29, 2014

\*To whom correspondence should be addressed.

Tel: +81-49-271-7246; Fax: +81-49-271-7984

E-mail: [h-mano@josai.ac.jp](mailto:h-mano@josai.ac.jp)

Hiroshi Mano, [h-mano@josai.ac.jp](mailto:h-mano@josai.ac.jp), 049-286-2233 (main phone number)

Sachie Nakatani, [s-nakata@josai.ac.jp](mailto:s-nakata@josai.ac.jp), 049-286-2233 (main phone number)

Yoshifumi Kimira, [kimira@josai.ac.jp](mailto:kimira@josai.ac.jp), 049-286-2233 (main phone number)

Mikiko Mano, [mmano@dent.meikai.ac.jp](mailto:mmano@dent.meikai.ac.jp), 049-285-5511 (main phone number)

Yuusuke Sekiguchi, [sekiguti@josai.ac.jp](mailto:sekiguti@josai.ac.jp), 049-286-2233 (main phone number)

Ryang-Hyock Im, [fs517@josai.ac.jp](mailto:fs517@josai.ac.jp), 049-286-2233 (main phone number)

Jun Shimizu, [jshimizu@josai.ac.jp](mailto:jshimizu@josai.ac.jp), 049-286-2233 (main phone number)

Masahiro Wada, [mwada@josai.ac.jp](mailto:mwada@josai.ac.jp), 049-286-2233 (main phone number)

The nucleotide sequences reported in this paper have been submitted to the DDBJ/GenBank/EBI Data Banks under accession number AB050983 (IF5)

Abbreviations used: ALP, alkaline phosphatase; FBS, fetal bovine serum; GAP, glyceraldehyde-3-phosphate dehydrogenase; IHC, immunohistochemistry; RT-PCR, Reverse-transcription polymerase chain reaction;

**Abstract** An IF5 cDNA was isolated by expression cloning from a mouse oocyte cDNA library. It encoded a protein of 250 amino acids, and the region of it encoding amino acids 1–137 showed 86.8% alignment with the anti-proliferative domain of BTG/TOB family genes. This gene is also termed BTG4 or PC3B. Transiently expressed IF5/BTG4 induced alkaline phosphatase activity in HEK293T and 2T3 cells. IF5/BTG4 mRNA was detected by reverse-transcription polymerase chain reaction in pharynx, larynx, trachea, oviduct, ovary, caput epididymis and testis, but not in lung, intestine or liver. Immunohistochemistry showed the IF5/BTG4 protein to be present in epithelial cells of the tongue, palate, pharynx, internal nose and trachea. Both protein and mRNA levels of IF5/BTG4 were reduced by aging when comparing 4-week-old mice with 48-week-old mice. Our findings suggest that IF5/BTG4 may be an aging-related gene in epithelial cells.

*Keywords:* IF5/BTG4; epithelium; oral; respiratory; aging

Running Head

Age-related decrease of IF5/BTG4 in epithelia

## 1   **Introduction**

2           The control of cell differentiation and/or proliferation is essential to cell  
3   function. A large number of signaling molecules are involved in cell differentiation  
4   and/or proliferation. Oct3/4, Sox2, c-Myc, and Klf4 are well known to be involved in  
5   cell differentiation and/or proliferation.<sup>1)</sup> However, other genes expressed in the oocyte  
6   may also control cell differentiation and/or proliferation, oogenesis and development.

7           Connective and epithelial tissues are basic tissue types in adult animals.<sup>2)</sup> The  
8   cell types in connective tissue and the genes that regulate their  
9   differentiation/proliferation have been well characterized. For example, adipocytes play  
10   a critical role in lipid metabolism and are controlled by PPAR $\gamma$ , while osteoblasts, which  
11   play a critical role in bone and mineral metabolism, are controlled by Runx2.<sup>3,4)</sup> The  
12   morphology of epithelia, such as simple, pseudostratified, stratified, and ciliated, is well  
13   known.<sup>2)</sup> Undifferentiated epithelial cells (epidermal stem cells) start to  
14   differentiate/proliferate as they move from the basal layer to the external layer of  
15   differentiated epithelial cells; however, there have been few reports characterizing the  
16   regulation of gene expression in epithelial cells.<sup>5,6)</sup>

17           Previously, we isolated the IF3/Oosp1 gene by expression cloning from a  
18   cDNA library made from mouse oocytes. This was based on the ability to induce  
19   alkaline phosphatase (ALP) activity in human embryonic kidney (HEK) 293T cells and  
20   mesenchymal cell lines because ALP is a marker of the differentiated state in  
21   mammalian cells. ALP is also used as a marker of the undifferentiated state in  
22   embryonic stem cells,<sup>7,8)</sup> and for the early-differentiated state of osteoblastic cells.<sup>9)</sup>  
23   IF3/Oosp1 is a secreted protein, and is expressed in both ovary and liver in adults. This  
24   gene may encode a secreted factor that regulates oogenesis and certain liver functions.  
25   IF3/Oosp1 induced osteoblastic and chondrogenic cell differentiation.<sup>10)</sup>

26           In the present study we isolated a gene, which we named IF5, by expression  
27   cloning from a cDNA library made from mouse oocytes. This gene was found to be a  
28   member of the TOB/BTG family of genes, which play a critical role in cell  
29   differentiation and/or proliferation through gene regulation.<sup>11-13)</sup> In this study, we  
30   investigated the effect of IF5/BTG4 on cell differentiation and cell proliferation. We  
31   also determined changes in the levels of IF5/BTG4 mRNA and protein with aging in  
32   tissues, including genital, oral and nasal organs.



## Materials and Methods

*Collection of oocytes.* Female C57BL/6J mice were superovulated with 5 IU pregnant mare serum gonadotropin followed 48 hours later by 2.5 IU human chorionic gonadotropin (hCG). The females were killed by cervical dislocation at 18 hours post-hCG injection, and their oviducts were removed and flushed with M2 medium (SIGMA-ALDRICH, Missouri, USA) using a flushing needle to recover newly ovulated eggs surrounded by cumulus cells. To collect pure oocytes, we removed the cumulus cells by hyaluronidase treatment and rinsed the oocytes in a different culture dish several times with M16 medium (SIGMA-ALDRICH, Missouri, USA).<sup>10)</sup> These oocytes were used for extraction of RNA.

*Mouse oocyte cDNA library.* Total RNA was purified from the mouse oocytes using TRIzol™ LS reagent (Invitrogen, California, USA).<sup>7)</sup> Total cDNA was then prepared from the total RNA using a SMART™ cDNA library construction kit (Clontech, California, USA). The cDNA fragments were subsequently inserted into the mammalian expression vector pcDNA3.1+ (Invitrogen, California, USA).<sup>14)</sup>

*Isolation of IF5/BTG4 from oocytes by an expression cloning method.* HEK293T cells were seeded in 35 mm cell-culture dishes at a density of  $1 \times 10^5$  cells/dish in Dulbecco's modified Eagle's medium (Gibco, California, USA) supplemented with 10% fetal bovine serum (FBS) and 100 U/mL penicillin and maintained at 37°C in a humidified atmosphere of 5% CO<sub>2</sub>. Fifteen hours after seeding, cells were transfected with the mouse oocyte cDNA library using FuGENE™ 6 (Promega, Wisconsin, USA).<sup>10)</sup> Three days after transfection, the cells were fixed with 20% formalin, rinsed with water, and stained for ALP activity with ALP-staining solution [1 mM naphthol AS-BI phosphate, 1 mM fast red violet LB salt, 0.05 M 2-amino-2-methyl-1-propanol (pH 9.8)] at 37°C for 15–30 min. Positively stained cells were harvested by micromanipulation and cDNAs in the cells were resuspended in TE buffer (10 mM Tris-HCl, 1 mM EDTA, pH 8.0). cDNAs were then amplified by polymerase chain reaction using a T7 promoter primer (5'-taatacgactcactataggg-3') and a pcDNA3.1 reverse priming site primer (5'-tagaaggcagctcgagg-3'). The purified PCR products were subcloned into pcDNA3.1+. Automated fluorescence DNA sequencing was performed using an ABI PRISM 310

genetic analyzer with BigDye terminator sequencing chemistry on double-stranded plasmid templates. Computer analysis of the sequences was then performed. Similarity searches were conducted using Blast and Fast algorithms against the GenBank, EMBL, and Swiss-Prot databases.<sup>10)</sup>

*Transfection of HEK293T or 2T3 cells with IF5/BTG4 plasmid for ALP activity staining and the MTT assay.* 2T3 cells were cultured in  $\alpha$  minimum essential medium (Gibco, California, USA) supplemented with 10% FBS and 100 U/mL penicillin. Cell cultures were maintained at 37°C in a humidified atmosphere of 5% CO<sub>2</sub>. Conditions for culturing HEK293T cells are described above. Fifteen hours after seeding ( $2 \times 10^3$  HEK293T cells/well or  $4 \times 10^3$  2T3 cells/well in a 96-well dish), cells were transfected with pcDNA3.1+ (Mock) or IF5/BTG4-pcDNA3.1+ (IF5/BTG4) using FuGENE™ 6. Briefly, a master transfection mixture containing 150  $\mu$ L of serum-free medium and 4.5  $\mu$ L of FuGENE™ 6 was incubated for 5 min at room temperature. Three  $\mu$ g of expression plasmid DNA and 1.5 mL of serum containing medium was then added. Two hundred  $\mu$ L of transfection medium was added to the cells. The effect of IF5/BTG4 on cell differentiation was assessed by ALP activity staining. Three days after transfection, the culture dish was stained for ALP activity with ALP-staining solution [1 mM naphthol AS-BI phosphate, 1 mM fast red violet LB salt, 0.05 M 2-amino-2-methyl-1-propanol (pH 9.8)] at 37°C for 15–30 min. The stained cells in the 96-well dish were digitally imaged by using a flatbed scanner to visualize ALP staining. The cells were measured at 540 nm for ALP activity using a WALLAC 1420 (Perkin Elmer, Massachusetts, USA) in a scanned-measurement mode, which measures 30 different points of a well. The effect of IF5/BTG4 on cell proliferation was assessed by MTT assays (Cell Counting Kit-HS; Dojindo, Kumamoto, Japan). Two days after transfection, the culture dish was washed with medium, and the MTT assay was carried out according to the manufacturer's protocol and with a plate reader at 540 nm.<sup>9,10)</sup>

*Reverse-transcription polymerase chain reaction (RT-PCR).* RNA was extracted from 4-week-old female and male mice and from 10- and 48-week-old male mice using

1 TRIzol™ (Invitrogen, California, USA). For RT-PCR analysis, we carried out oligo-dT-  
2 primed reverse transcription on aliquots of total RNA using SuperScript II (Invitrogen,  
3 California, USA). A 1/20<sup>th</sup> fraction of the single-stranded cDNA products was used for  
4 each PCR amplification with TaKaRa Ex Taq (Takara, Shiga, Japan). IF5 gene-specific  
5 primers for PCR were: 5'-caccctgactgccctccaag-3' (IF5-O-F1) and 5'-  
6 gctggtctgcgtgcaaggaca-3' (IF5-O-R1). The reaction efficiencies and the initial amount of  
7 RNA template in each reaction were assessed using primers specific for mouse  
8 glyceraldehyde-3-phosphate dehydrogenase (GAP, 5'-ttgacctcaactacatgg-3' and 5'-  
9 atgaggtccaccaccctg-3').<sup>10)</sup> The  $\beta$ III-tubulin gene was used as a marker for ciliated  
10 epithelium (TBb3, 5'-cccagcggcaactatgta-3' and 5'-gtaagtggggcgaagccg-3').<sup>15)</sup> The  
11 following PCR conditions were used: 1 cycle at 94°C for 5 min followed by 20 cycles  
12 for GAP, 25 cycles for TBb3, and 38 cycles for IF5/BTG4, consisting of denaturation  
13 (1 min at 94°C), annealing (1 min at 58°C), and elongation (3 min at 72°C). One-fourth  
14 of each PCR product was electrophoresed through a 1.5% agarose gel and visualized by  
15 staining with ethidium bromide. All gels were digitally imaged using a flatbed scanner  
16 and analyzed using Adobe PhotoShop Elements software. Within each series, all  
17 adjustments were made in parallel to all compared gels. The band intensities of these  
18 digital images were determined using NIH ImageJ software for gels from at least three  
19 different experiments. The signals were normalized to those of GAP transcripts.

20  
21 *Immunohistochemistry (IHC)*. Mice were injected with an overdose of pentobarbital  
22 (100 mg/kg), followed by heparin (10 U/kg). They were then perfused transcardially  
23 with 15 mL 4% paraformaldehyde contained in 0.1 M phosphate buffer (PB; pH 7.4).  
24 After perfusion, tissues were dissected and then fixed for 12–16 h in 4%  
25 paraformaldehyde in PB. Then the tissues were cryoprotected for 16–20 h in PB  
26 containing 12.5% sucrose and then for the same time in PB containing 25% sucrose.  
27 Serial sections of 5–10  $\mu$ m thickness were prepared using a LEICA CM3050S, mounted  
28 serially on silane-coated glass slides, and air-dried. The sections were next washed in  
29 0.01 M phosphate-buffered saline (PBS) and incubated with 0.3% H<sub>2</sub>O<sub>2</sub> in methanol for  
30 30 min. After a rinse with PBS, they were blocked for 1 h at room temperature with  
31 PBS containing 10% FBS. Subsequently, the sections were incubated for 30 min at  
32 room temperature with a 1:100 dilution of epitope-affinity-purified polyclonal rabbit

1 anti-IF5/BTG4 antibody (epitope: 40–50 amino acid region of mouse IF5/BTG4;  
2 Transgenic Co., Kumamoto, Japan) in PBS containing 10% FBS. After rinsing in PBS  
3 containing 0.02% Tween 20 (PBS-T), the sections were blocked with 10% FBS/PBS for  
4 1 h at room temperature. Thereafter they were incubated with a secondary antibody  
5 (1:100 goat anti-rabbit IgG (H+L) HRP Conjugate, ZyMax™, ZYMED, California,  
6 USA) in 10% FBS/PBS for 30 min at room temperature. After a rinse in PBS-T, they  
7 were finally treated with 3,3'-diaminobenzidine (DAB) solution (Dako, Glostrup,  
8 Denmark) for 10 min at room temperature. Negative control experiments, in which the  
9 primary antibody was omitted, revealed no DAB staining at the site of the target antigen.  
10 After a final rinse with PBS, sections were stained with Mayer's hematoxylin.  
11 Microscopy images were collected using Lumina Vision software (Mitani Corporation,  
12 Japan).

13 All animal experiments were approved by the Institutional Animal Care and  
14 Use Committee of Josai University.

15  
16 *Statistical analysis.* Results are presented as means  $\pm$  standard deviation (SD).  
17 Statistical analysis was performed using Student's t-test. Values of  $p < 0.05$  were  
18 considered significant.



## Results

*Cloning a IF5/BTG4 cDNA.* To identify genes involved in the regulation of cell differentiation and/or cell proliferation, we performed expression cloning using an oocyte cDNA library [34]. HEK293T cells express the SV40 large T antigen, and normal HEK293T cells do not express ALP. ALP is used as a marker of the differentiated state in some cells, such as embryonic stem cells, osteogenic cells and chondrogenic cells. Therefore, we screened the mouse oocyte cDNA library for cDNAs that would induce ALP activity in the HEK293T cells.<sup>10)</sup>

Clone 005, which we named IF5 (IF5), had a cDNA insert of approximately 1377 nucleotides (nt) that contained an entire open reading frame (ORF), with a 5'-UTR of 228 nt and a 3'-UTR of 396 nt. The predicted protein product encoded by the ORF was 250 amino acids in length, with a calculated molecular mass of approximately 28.6 kDa (Fig. 1A).

The protein sequence deduced from the IF5 cDNA, when compared with sequences in the PIR, SWISS-PROT, DAD, and PDBSH protein databases by using BLAST, was identical to the mouse BTG4/PC3B protein. BTG4/PC3B/IF5 was reported independently by F. Tirone et al (BC066811), P. Buanne et al (AJ005120), and H. Mano (AB050983, only published in the database). F. Tirone et al. identified BTG4/PC3B by exhaustive cloning to identify complete ORF cDNAs from a mouse cDNA library.<sup>16)</sup> P. Buanne et al identified BTG4/PC3B by screening the EST database for similar, but not identical sequences to those of TOB/BTG family members.<sup>11)</sup> Our sequence (AB050983) is the longest in terms of its 3'-UTR compared with BC066811 and AJ005120 sequences, and is identical to that of Btg4 (NT 039473.3; official name of its genome location), although some polymorphisms have been identified: BC066811 (L247P) and AJ005120 (I37V, I158V). BTG4/PC3B is a member of the BTG/TOB anti-proliferative gene family. Their members have a highly homologous N terminal domain (Fig.1 B).

*Effect of IF5/BTG4 on ALP activity and cell proliferation in HEK293T and 2T3 cells.* To analyze IF5/BTG4 function, we transfected HEK293T and 2T3 cells with the mouse IF5/BTG4-pcDNA3.1+ or pcDNA3.1+. Transiently expressed IF5/BTG4 induced ALP

activity in HEK293T and 2T3 cells after 3 days in culture (Fig. 2. A, B, C, D). However, transiently expressed IF5/BTG4 did not affect cell proliferation of HEK293T or 2T3 cells after 2 days in culture (Fig. 2. E, F). These observations indicate that IF5/BTG4 might affect the cell differentiation stage of HEK293T and 2T3 cells.

*Expression of IF5/BTG4 mRNA in adult mouse tissues.* IF5/BTG4 mRNA was highly expressed in the pharynx, larynx, trachea and ovary, as determined by RT-PCR using the IF5-O-F1 and IF5 -O-R1 primer set (Fig. 3A). We also analyzed the expression of IF5/BTG4 in the genital system by RT-PCR. IF5/BTG4 mRNA was detected in ciliated organs, such as the oviduct, caput epididymis, and testis (Fig. 3B and C). We confirmed the sequence of the product to be that of the mouse IF5/BTG4 gene and thus concluded that IF5/BTG4 might play a role in ciliated epithelium.

*Down-regulation of IF5/BTG4 expression with aging in adult trachea.* Changes in the function and structure of ciliated epithelium in the trachea have been reported to be related to aging.<sup>17)</sup> We therefore examined the effect of aging on the levels of IF5/BTG4 mRNA in mouse trachea using RT-PCR. The level of TBb3 mRNA was slightly reduced with aging (Fig. 4A and B). Moreover, the level of IF5/BTG4 mRNA was dramatically decreased even in the trachea of 10-week-old mice compared to 4-week-old mice, and it became undetectable in the trachea of 48-week-old mice (about one-third) (Fig. 4A and B).

*Down-regulation of IF5/BTG4 protein levels with aging in oral and nasal cavities.* We confirmed the effect of aging on the level of IF5/BTG4 protein in mouse ciliated epithelium in oral and nasal cavities. BTG4 mRNA is expressed in mouse olfactory epithelium.<sup>11)</sup> The use of the epitope-affinity-purified polyclonal rabbit anti-IF5/BTG4 antibody clarified the distribution of IF5/BTG4 protein in these locations. IF5/BTG4 immunoreactivity was stained brown by the DAB chromogen, and the cell nuclei were stained blue or violet by Mayer's hematoxylin. The IF5/BTG4 protein was detected in epithelial cells in the lip, follicle, palate, tongue, olfactory organ, and nasopharynx (Fig. 5). However, we did not detect the protein in epithelial cells in the esophagus by IHC (data not shown). The IF5/BTG4 protein was clearly stained in epithelial cells in the

1 palate (A), nasopharynx (C) and trachea (E) in 4-week-old mice. However, its staining  
2 was weak in these tissues from 48-week-old animals (Fig. 6). These data suggest that  
3 the level of IF5/BTG4 protein decreased with increasing age, similarly to its mRNA  
4 levels.

5

6

## Discussion

We cloned the full-length cDNA of mouse IF5/BTG4, which belongs to the BTG/TOB gene family, from a mouse oocyte cDNA library. We showed that ALP activity is induced in HEK293T and 2T3 cells transfected with an IF5/BTG4 expression plasmid. However, cell proliferation of HEK293T or 2T3 cells was not affected. 2T3 cells are able to differentiate into both osteoblasts and adipocytes<sup>18)</sup> and ALP is an early differentiation stage maker of osteogenic cells.<sup>9)</sup> On the other hand, ALP is a non-differentiation maker in embryonic stem cells.<sup>7,8)</sup> Also, increased ALP activity and decreased protein-kinase C activity is related to differentiation of a human leukemia cell line.<sup>19)</sup> These data suggest that IF5/BTG4 may induce osteogenesis and control cell differentiation in 2T3 cells.

BTG/TOB proteins might be factors that control the cell cycle, cell differentiation and cell senescence.<sup>13)</sup> BTG2, BTG3 and BTG4 exert anti-proliferative effects and are targets of p53. BTG4 may also be involved in epigenetic actions in development and in disease pathogenesis.<sup>20)</sup> Phosphorylated TIS21/BTG2 inhibits phosphorylated mitotic regulators resulting in repression of cell proliferation and induction of cell death.<sup>21)</sup> It is reported that BTG1 mRNA expression levels decrease with progression of ovarian carcinomas<sup>22)</sup> and that TIS21/BTG2 induces cellular senescence,<sup>21)</sup> but that loss of BTG3 induces cellular senescence.<sup>23)</sup> TOB1 plays an important role in skeletal muscle development.<sup>24)</sup> The roles of TOB/BTG gene family members are very controversial.

The mRNA and protein expression of IF5/BTG4 in normal adult animals has not been fully elucidated. IF5/BTG4 mRNA was expressed in mouse genital, oral, and respiratory tissues. IF5/BTG4 protein was detected in oral and respiratory epithelial cells. These results suggest that this gene might have a physiological function in genital, oral, and respiratory tissues. IF5/BTG4 might play a critical role in ciliated cells in adults. The mRNA profile of BTG4 in mouse olfactory development has been reported.<sup>11)</sup> We therefore clarified that aging affects the levels of IF5/BTG4 mRNA and protein in oral and respiratory epithelia. IF5/BTG4 mRNA was highly expressed in the trachea of juvenile mice (4 weeks old), and expressed at low levels in adult mice (10 weeks old). IF5/BTG4 mRNA could not be detected in aged mice (48 weeks old) by RT-PCR. Moreover, we showed that the IF5/BTG4 protein was absent from trachea and

nasal pharynx epithelial cells of older mice; it was not expressed in these non-ciliated cells. These data suggest that the decrease of IF5/BTG4 levels may affect function and maintenance of oral and respiratory epithelial cells.

Aging affects growth, reproduction, and somatic survival in the animal body. Recent studies suggest that aging is caused not by gene programming but by ecological factors, such as stress and food.<sup>25-27)</sup> However, some aging-related genes were detected in Werner syndrome patients and in older animals; and moreover, the activity of genes such as metallothionein, basic helix-loop-helix upstream stimulatory factor-1 and sonic hedgehog, that regulates the development of taste buds in the oral epithelium was reported to be aging related.<sup>28-31)</sup> However, our current data do not clarify the relationship between IF5/BTG4 and aging. Further study is needed to clarify the function of IF5/BTG4 in aging in oral and respiratory cavities.

In this study, IF5/BTG4 was shown to be an aging-related gene, whose expression decreases with aging. Furthermore, IF5/BTG4 regulates cell differentiation in the oral and respiratory cavities and is involved in oogenesis and spermatogenesis.

## Acknowledgments

We express our gratitude to Prof. Masahiro. Kumegawa (Meikai University) for useful comments and to Prof. Lynda F. Bonewald (University of Missouri-Kansas City) for the generous gift of 2T3 cells.

## References

- 1) Takahashi K, and Yamanaka S. Induction of pluripotent stem cells from mouse embryonic and adult fibroblast cultures by defined factors. *Cell*, **126**, 663-676 (2006).
- 2) Vasiliev JM. The role of connective tissue proliferation in invasive growth of normal and malignant tissues: a review. *Br. J. Cancer.*, **12**, 524–536 (1958).
- 3) Tontonoz P, Hu E, and Spiegelman BM. Stimulation of adipogenesis in fibroblasts by PPAR gamma 2, a lipid-activated transcription factor. *Cell*, **79**, 1147-1156 (1994).
- 4) Komori T, Yagi H, Nomura S, Yamaguchi A, Sasaki K, Deguchi K, Shimizu Y, Bronson RT, Gao YH, Inada M, Sato M, Okamoto R, Kitamura Y, Yoshiki S, and Kishimoto T. Targeted disruption of Cbfa1 results in a complete lack of bone formation owing to maturational arrest of osteoblasts. *Cell*, **89**, 755-764 (1997).
- 5) Alonso L, and Fuchs E. Stem cells of the skin epithelium. *Proc. Natl. Acad. Sci. USA.*, **100**, 11830-11835 (2003).
- 6) Tumbar T, Guasch G, Greco V, Blanpain C, Lowry WE, Rendl M, and Fuchs E. Defining the epithelial stem cell niche in skin. *Science*, **303**, 359-363 (2004).
- 7) O'Connor MD, Kardel MD, Iosfina I, Youssef D, Lu M, Li MM, Vercauteren S, Nagy A, and Eaves CJ. Alkaline phosphatase-positive colony formation is a sensitive, specific, and quantitative indicator of undifferentiated human embryonic stem cells. *Stem Cells*, **26**, 1109-1116 (2008).
- 8) Saito S, Liu B, and Yokoyama K. Animal embryonic stem (ES) cells: self-renewal, pluripotency, transgenesis and nuclear transfer. *Hum. Cell*, **17**, 107-15 (2004).
- 9) Kimira Y, Ogura K, Taniuchi Y, Kataoka A, Inoue N, Sugihara F, Nakatani S, Shimizu J, Wada M, and Mano H. Collagen-derived dipeptide prolyl-hydroxyproline promotes differentiation of MC3T3-E1 osteoblastic cells. *Biochem. Biophys. Res. Commun.*, **453**, 498-501 (2014).
- 10) Mano H, Nakatani S, Aoyagi R, Ishii R, Iwai Y, Shimoda N, Jincho Y, Hiura H, Hirose M, Mochizuki C, Yuri M, Im RH, Funada-Wada U, and M. Wada. IF3, a novel cell-differentiation factor, highly expressed in murine liver and ovary. *Biochem. Biophys. Res. Comm.*, **297**, 323-328 (2002).
- 11) Buanne P, Corrente G, Micheli L, Palena A, Lavia P, Spadafora C, Lakshmana MK, Rinaldi A, Banfi S, Quarto M, Bulfone A, and Tirone F. Cloning of PC3B, a novel

1 member of the PC3/BTG/TOB family of growth inhibitory genes, highly expressed in  
2 the olfactory epithelium. *Genomics*, **68**, 253-263 (2000).

3 12) Yoshida Y, Tanaka S, Umemori H, Minowa O, Usui M, Ikematsu N, Hosoda E,  
4 Imamura T, Kuno J, Yamashita T, Miyazono K, Noda M, Noda T, and Yamamoto T.  
5 Negative regulation of BMP/Smad signaling by Tob in osteoblasts. *Cell*, **103**, 1085-  
6 1097 (2000).

7 13) Dong W, Tu S, Xie J, Sun P, Wu Y, and Wang L. Frequent promoter  
8 hypermethylation and transcriptional downregulation of BTG4 gene in gastric cancer.  
9 *Biochem. Biophys. Res. Comm.*, **387**, 132-138 (2009).

10 14) Mano H, Kimura C, Fujisawa Y, Kameda T, Watanabe-Mano M, Kaneko H, Kaneda  
11 T, Hakeda Y, and Kumegawa M. Cloning and function of rabbit peroxisome  
12 proliferator-activated receptor delta/beta in mature osteoclasts. *J. Biol. Chem.*, **275**,  
13 8126-8132 (2000).

14 15) Woo K, Jensen-Smith HC, Luduena RF, and Hallworth R. Differential synthesis of  
15 beta-tubulin isotypes in gerbil nasal epithelia. *Cell Tissue Res.*, **309**, 331-335 (2002).

16 16) Mammalian Gene Collection Program Team. Generation and initial analysis of more  
17 than 15,000 full-length human and mouse cDNA sequences. *Proc. Natl. Acad. Sci. USA*,  
18 **99**, 16899-16903 (2002).

19 17) Campisi J. Senescent cells, tumor suppression, and organismal aging: good citizens,  
20 bad neighbors. *Cell*, **120**, 513-522 (2005).

21 18) Chen D, Ji X, Harris MA, Feng JQ, Karsenty G, Celeste AJ, Rosen V, Mundy GR,  
22 and Harris SE. Differential roles for bone morphogenetic protein (BMP) receptor type  
23 IB and IA in differentiation and specification of mesenchymal precursor cells to  
24 osteoblast and adipocyte lineages. *J. Cell Biol.*, **142**, 295-305 (1998).

25 19) Yung BY, Hsiao TF, Wei LL, and Hui EK. Sphinganine potentiation of dimethyl  
26 sulfoxide-induced granulocyte differentiation, increase of alkaline phosphatase activity  
27 and decrease of protein kinase C activity in a human leukemia cell line (HL-60).  
28 *Biochem. Biophys. Res. Commun.*, **199**, 888-896 (1994).

29 20) Toyota M, Suzuki H, Sasaki Y, Maruyama R, Imai K, Shinomura Y, and Tokino T.  
30 Epigenetic silencing of microRNA-34b/c and B-cell translocation gene 4 is associated  
31 with CpG island methylation in colorectal cancer. *Cancer Res.*, **68**, 4123-4132 (2008).

32 21) Lim IK. TIS21 (/BTG2/PC3) as a link between ageing and cancer: cell cycle

regulator and endogenous cell death molecule. *J. Cancer. Res. Clin. Oncol.*, **132**, 417-426 (2006).

22) Zhao Y, Gou WF, Chen S, Takano Y, Xiu YL, and Zheng HC. BTG1 expression correlates with the pathogenesis and progression of ovarian carcinomas. *Int. J. Mol. Sci.*, **14**, 19670-19680 (2013).

23) Lin TY, Cheng YC, Yang HC, Lin WC, Wang CC, Lai PL, and Shieh SY. Loss of the candidate tumor suppressor BTG3 triggers acute cellular senescence via the ERK-JMJD3-p16(INK4a) signaling axis. *Oncogene*, **31**, 3287-3297 (2012).

24) Yuan J, Cao JY, Tang ZL, Wang N, and Li K. Molecular characterization of Tob1 in muscle development in pigs. *Int. J. Mol. Sci.*, **12**, 4315-4326 (2011).

25) Kyng KJ, May A, Kolvraa S, and Bohr VA. Gene expression profiling in Werner syndrome closely resembles that of normal aging. *Proc. Natl. Acad. Sci. USA*, **100**, 12259-12264 (2003).

26) Baffert F, Thurston G, Rochon-Duck M, Le T, Brekken R, and McDonald DM. Age-related changes in vascular endothelial growth factor dependency and angiopoietin-1-induced plasticity of adult blood vessels. *Circ. Res.*, **94**, 984-992 (2004).

27) Kirkwood TBL. Understanding the odd science of aging. *Cell*, **120**, 437-447 (2005).

28) Seta Y, Toyono T, Takeda S, and Toyoshima K. Expression of Mash1 in basal cells of rat circumvallate taste buds is dependent upon gustatory innervation. *FEBS letter*, **444**, 43-46 (1999).

29) Andrews GK, Lee DK, Ravindra R, Lichtlen P, Sirito M, Sawadogo M, and Schaffner W. The transcription factors MTF-1 and USF1 cooperate to regulate mouse metallothionein-I expression in response to the essential metal zinc in visceral endoderm cells during early development. *EMBO J.*, **20**, 1114-1122 (2001).

30) Stone LM, Tan SS, Tam PPL, and Finger TE. Analysis of cell lineage relationships in taste buds. *J. Neurosci.*, **22**, 4522-4529 (2002).

31) Liu HX, MacCallum DK, Edwards C, Gaffield W, and Mistretta CM. Sonic hedgehog exerts distinct, stage-specific effects on tongue and taste papilla development. *Dev. Biol.*, **276**, 280-300 (2004).



Fig. 1. Cloning of the IF5/BTG4 cDNAs. (A) Nucleotide and deduced amino acid sequences of mouse IF5/BTG4 cDNA from oocytes. The deduced amino acid sequence of IF5/BTG4 indicates a 250 amino acid protein. The homology domain is indicated by the box, and the epitope sequence used for generating the antibody is underlined (amino acids 40–50). (B) BTG/TOB family of anti-proliferative genes. The homology domain, nuclear localization signal (NLS), and proline (P) and glutamine (Q)-rich sequences are indicated.

Fig. 2. Effect of IF5/BTG4 on ALP activity and cell proliferation in HEK293T and 2T3 cells. Photographs from ALP staining as typical cultures of HEK293T (A) and 2T3 cells (B) treated with pcDNA3.1+ (Mock) or IF5/BTG4-pcDNA3.1+ (IF5/BTG4). The ratio of ALP activity in HEK293T (C) and 2T3 cells (D) transfected with pcDNA3.1+ (Mock) or IF5/BTG4-pcDNA3.1+ (IF5/BTG4) was calculated after measurement with a plate reader at 540 nm. The ratio of MTT assays in HEK293T (E) and 2T3 cells (F) treated with pcDNA3.1+ (Mock) or IF5/BTG4-pcDNA3.1+ (IF5/BTG4) was calculated after measurement with a plate reader at 540 nm. Data are presented as means  $\pm$  SD (n=3), \*P<0.05 compared to mock-transfected cells.

Fig. 3. RT-PCR analysis of IF5/BTG4 mRNA in adult tissues. Total RNA was isolated from adult female mouse tissues (A) and from adult female and male genital tissues (B and C). GAP was used as an indicator of the amount of RNA used for analysis. The experiment was performed three times, with similar results each time.

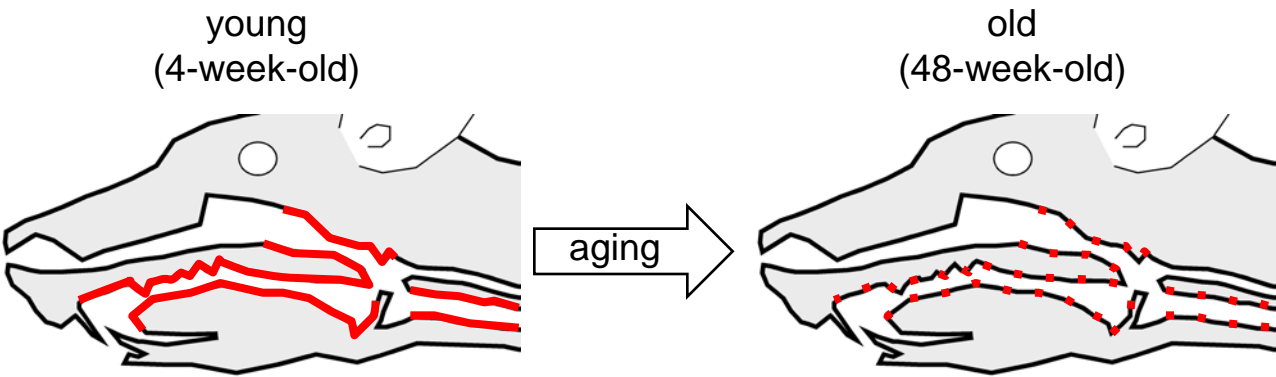
Fig. 4. Effect of aging on IF5/BTG4 mRNA levels in adult trachea. Total RNA was isolated from the trachea of 4-, 10-, and 48-week-old mice and RT-PCR analysis performed. TBb3 was used as a positive control for expression in ciliated trachea. The gel electrophoresis patterns of the PCR products (A), and densitometric analysis were performed as described in the Materials and Methods. The signals obtained from these digitally imaged gels in at least three different experiments (n=6) were normalized relative to GAP mRNA levels, as shown in the graph (B). Data are presented as means  $\pm$  SD (n=6), \*P<0.05 compared to 4-week-old mice.

Fig. 5. IHC analysis of IF5/BTG4 protein distribution in mouse oral and nasal cavities. Low-magnification view of sagittal section of head and neck (A). High-magnification view of lip (B), olfactory organ (C), nasopharynx (D), and oral cavity (E) from the same section shown in “A”. The analysis was performed using three different mice, with similar results each time. Lip (L), olfactory organ (O), tongue (T), palate (P), nasopharynx (NP), oral cavity (OC), and brain (B) are indicated.

Fig. 6. Effect of aging on IF5/BTG4 protein levels in oral and respiratory epithelia. IHC analysis was performed using an anti-IF5/BTG4 antibody and sections prepared from 4- (A, C, E) and 48- (B, D, F) week-old mice. High-magnification views of palate (A, B), nasopharynx (C, D), and trachea (E, F) are shown. The experiment was performed using three different mice, with similar results each time.

IF5/BTG4 was shown to be an aging-related gene, whose expression decreases with aging in the oral and respiratory cavities. Furthermore, IF5/BTG4 regulates cell differentiation.

IF5/BTG4 EXPRESSION




A

```

5' GGC CAT TAT9 GGC GGG18 GAA ATA GGT ATG27 GGT CAG AGT36 TGG CAA CAA45 GTA GTG TGG54
CTG GCT63 CTC TAA CTT TGG ACC ACT TTT TGT AGA GAC CAG AGA99 CTT TCT AGC108
AAG TGT117 AAT GTG TTT126 TTA ATA ATC135 TTT TAC TGT144 GCA GTT TTG153 GCC ACA TTT162
TCC AAC171 GGC GGT CCT CTG AAG CCT180 GAA TAT TTG189 ACT CTA TGT198 CTC TAC ACA207
TGC TTT216 GGA ATC225 ATG AGA234 GAC GAA243 ATT GCA ACA252 GTT TTT261 GTC ACA270
M R D E I A T A V F F V T R279
TTC GTG279 AAG CAT288 AAA CTG297 ACT CAA306 ATA GAA315 TTT GCA324
L V K K H E K L S T Q Q I E F A L333
AAG CTG333 ATG ACC ATC342 TTT GAA AAG351 TAC AGA360 CAC TGG369 CAC CCT GAC378
K L M T I L F E K Y R G H N H F D C387
CCT TCC387 AAG GGG CAG396 GCT TTC405 AGG TGT ATC414 AAC ATA423 GAG AAT432
P S K G Q A F R C I R I N N N E N K441
GAC CCT441 GTT TTA GAA450 GCT TGT GCT459 GAG AGT468 GTG AAT477 TTT CAT486
D P V L E R A C A E S H V N F F H L495
GGA CTT495 CCA AAG AAG504 ACC ATA513 GTC GAT522 TAT GAG531 TGC TGT540
G L P K E M T I N V D B Y E C C R549
TAT GGT549 GAG AAA AAG CAT558 CCC TTT ACA ATT567 TCT TCT576 TTT AAA GGT585 AGA TGG594
V G E K K H P F T I A S F K G R W E603
AAC TGG603 GAG TTG GCT CAG CAT612 GTC AGC TGT GCA GTT621 AAC AGA GGC630 ACG GGA639
N W E L A Q H V S C A V N R A T G D648
TGC TCC657 GGC ACA666 TCT GAT675 GAA AGC684 AGC AGG GAG693 GCC CAG702
C S S G T S S D E S C S R E A Q I711
ATC CCC711 AAG GTG AAC720 CCA AAG729 GTC TAC CAG GTT738 GAA AAT747 TTC AAA756
K V N N P E K Q N E N F K Q C765
TCA TTG765 CAG CCG TGG TTC774 TGC CTC783 CGT AGA792 CAT TTG801 GCA GAT GGT810
S L Q P W F C L P R R K H L A D G R819
GGG TTC819 CCG GGG GCT TGC828 CAC CCA GTG837 AAG AGC846 AAG TCT855 AAG TGG864
G F L P G A A C H P V P K S S K W C873
CGG CCA873 GCT TCG CGC882 GTG GAC AGA891 TAT CAC900 TGG GTC909 CAA CTG918
R P A S R V D R Y H W V N Q L F927
AGT GGT927 CAG ACA CCA CCA GGA GAG936 CCT GGA GAA GAG945 GGC TTG TCT954 TCC CTA963
S G Q T A P G E P G E E A L S S L K972
CAA AAA981 TGA990 GGC TAA999 CAA GAA1008 ATG CCC CCA GTA1017 AAA AAT1026 GGC TGT1035
Q K * 250
AGG AAT1035 GGG ACA GAA GGC TGT1044 CCT TGC ACG1053 ACC AGC1062 ACC AGC1071 TGA CTT1080
GCT ACT1089 TTT AAT TCT TAT TTA ACT1098 TTA TGT AAA ATT1107 TTA TGA ACA CTA GTG AAT1116
ATA GGT1125 GGC TAG AAA AGT GAT AGA1134 ACA GAG ATG TTG1143 CCG GTG ATA AAA TAA AAT1152
GAA TTA TGG GAA GGA AGA CTT1161 GAA ATA AAT ACT CTT1170 GTG TTT TTA ACA AAC TTT1179
TAG TTC1188 AGT TTG TTA GAC AGT1197 TTT AAG TCT TGT1206 TTT AAT CAT TGT TTT AAA1215
AGT AGG TTT TCA ACT AAG GAA GAT TGA1224 TCC TCA AAA AAA AAA AAA AAA AAA1233
AAA AAA1242 AAG ATG TCG TCG1251 CCG CCG1260 TCG1269 CCG1278 CCG1287 CCG1296 CCG1305
1314 1323 1332 1341 1350

```

B

IF5/BTG4  250 a.a.ANA/BTG3  P 252 a.a.Tob  345 a.a.BTG1  171 a.a.PC3/TIS21/BTG2  158 a.a.

